NASA TN D-350

TECHNICAL NOTE
D-350

HEAT TRANSFER TO SURFACES OF FINITE CATALYTIC ACTIVITY IN FROZEN DISSOCIATED HYPERSONIC FLOW

By Paul M. Chung and Aemer D. Anderson

Ames Research Center
Moffett Field, Calif.

NATIONAL AERONAUTICS AND SPACE ADMINISTRATION
WASHINGTON

January 1961

NATIONAL AERONAUTICS AND SPACE ADMINISTRATION

TECHNICAL NOTE D-350

HEAT TRANSFER TO SURFACES OF FINITE CATALYTIC ACTIVITY IN FROZEN DISSOCIATED HYPERSONIC FLOW

By Paul M. Chung and Aemer D. Anderson

SUMMARY

The heat transfer due to catalytic recombination of a partially dissociated diatomic gas along the surfaces of two-dimensional and axisymmetric bodies with finite catalytic efficiencies is studied analytically. An integral method is employed resulting in simple yet relatively complete solutions for the particular configurations considered.

A closed form solution is derived which enables one to calculate atom mass-fraction distribution, therefore catalytic heat transfer distribution, along the surface of a flat plate in frozen compressible flow with and without transpiration.

Numerical calculations are made to determine the atom mass-fraction distribution along an axisymmetric conical body with spherical nose in frozen hypersonic compressible flow. A simple solution based on a local similarity concept is found to be in good agreement with these numerical calculations. The conditions are given for which the local similarity solution is expected to be satisfactory.

The limitations on the practical application of the analysis to the flight of the blunt bodies in the atmosphere are discussed. The use of boundary-layer theory and the assumption of frozen flow restrict application of the analysis to altitudes between about 150,000 and 250,000 feet.

INTRODUCTION

Surface reaction, long a subject of interest in the chemical industry, has become important in aerodynamics in connection with high altitude hypersonic flight. When the flight conditions are such that

the flow of dissociated air past the body is almost chemically frozen, heat transfer to the body is strongly influenced by the amount of catalytic recombination at the wall. With noncatalytic walls, the chemical energy of the flow does not contribute to the heat transfer at all and, conversely, with highly catalytic walls the heat transfer is approximately the same as that which occurs across an equilibrium boundary layer. Thus, when the air is completely dissociated the heat transfer may vary with the catalytic activity of the wall from about 25 percent to about 100 percent of equilibrium heat transfer.

Boundary-layer theory was first applied to surface chemical reaction problems by Chambré and Acrivos (ref. 1). Since then many people, such as Chambré, Acrivos, Rosner, Goulard, Anderson, and Chung (refs. 2 through 8) have studied the problem for various applications using different approaches. The specific solutions obtained are for

1. The incompressible flow over a flat plate upon which an arbitrary order chemical reaction[1] occurs (refs. 1 through 5).

2. The compressible flow over a flat plate upon which first-order chemical reaction takes place (ref. 8).

3. The first-order chemical reaction at the stagnation point in a dissociated hypersonic flow without mass transfer (ref. 6), and with mass transfer (ref. 7).

In this paper, an integral method will be used to obtain catalytic heat-transfer predictions for (1) a flat plate in frozen compressible flow with and without transpiration and (2) an axisymmetric conical body with a spherical nose in frozen hypersonic compressible flow without transpiration.

The effect of mass transfer is included in the present analysis because it may be used for cooling purposes in a hypersonic flight and also because there is mass transfer at the surface when the surface participates in the chemical reaction.

SYMBOLS

B_1, B_2 constants for equation (51) given in table, page 16

C $\left(\frac{\rho_{w,o}\mu_{w,o}}{\rho_{e,o}\mu_{e,o}}\right)^{0.2}$

[1]The reaction rate at the wall is an arbitrary function of the surface concentration of the reactant.

$\overline{C}$	parameter defined by equation (9)
c	mass fraction
c_p	frozen specific heat at constant pressure
D	coefficient of binary diffusion
F	Blasius stream function used in equation (63)
F_1	momentum integral defined by equation (39)
F_2	concentration integral defined by equation (41)
G	reaction parameter defined by equation (49)
$\overline{G}$	$\frac{G}{\sqrt{\beta_0}}$
h	frozen total enthalpy defined by equation (6)
Δh^0	heat of recombination
$J_{1,w}$	mass flux of atoms to the wall
K_1	parameter defined by equation (53)
$\overline{K}_1$	$\frac{K_1}{\sqrt{\beta_0}}$
K_2	parameter defined by equation (54)
K_3	parameter defined by equation (55)
k	frozen thermal conductivity of gas
k_w	specific rate constant for surface recombination
L	reference length (see fig. 1)
M	molecular weight
M_∞	free-stream Mach number
m	$\frac{c_1}{c_{1,e}}$
p	pressure
Pr	Prandtl number

q total heat-transfer rate toward the wall per unit area

q_c convective heat-transfer rate toward the wall per unit area

q_d heat transfer rate per unit area by atom recombination at the surface

R universal gas constant

r distance from the axis of symmetry to a point on the surface (see fig. 1)

Re Reynolds number, $\frac{\rho u_\infty L}{\mu}$

s streamwise independent variable defined by equation (7)

Sc Schmidt number, $\frac{\mu}{\rho D}$

T absolute temperature

t independent variable defined by equation (8)

U $\frac{u}{u_e} = \frac{\partial \Psi}{\partial t}$

u x component of velocity

V $\frac{-\partial \Psi}{\partial s}$

v y component of velocity

X $\frac{x}{L}$

x streamwise distance along the surface

y distance normal to surface

Z mass rate of collision of atoms with the wall

z variable defined by equation (65)

β $\frac{du_e}{dx}$

Γ transpiration parameter defined by equation (38)

γ	surface catalytic efficiency
δ	boundary-layer thickness
δ_t	modified boundary-layer thickness defined by equation (36)
ϵ	$\begin{cases} 0 \text{ for two-dimensional bodies} \\ 1 \text{ for axisymmetric bodies} \end{cases}$
η	$\frac{t}{\delta_t}$ defined by equation (36)
θ	nose angle
λ	parameter defined by equation (37)
μ	dynamic viscosity
ν	kinematic viscosity
ξ	dummy variable
ρ	density
σ	$\frac{m_w}{m_{w,o}} = \frac{C_{1,w}}{C_{1,w,o}}$
Φ	shape factor defined by equation (50)
Δ	shock layer thickness
$\overline{\Phi}$	$\sqrt{\beta_o}\,\Phi$
χ	equilibrium mole fractions
Ψ	stream function defined by equations (14) and (15)
Ω	parameter defined by equation (81)

Subscripts

E	equilibrium
e	edge of boundary layer
i	ith species

m mixture

w wall

o leading edge of flat plate or stagnation point of sphere

1 atoms

2 molecules

∞ free stream

Superscript

' differentiation with respect to s except for equation (63)

SIMPLIFICATION OF BOUNDARY-LAYER EQUATIONS

The classical laminar boundary-layer theory is used in the present paper. The fluid is considered to be a partially dissociated diatomic gas of constant Schmidt number and it is assumed to be frozen in this state throughout the entire flow field. The actual range of flight conditions in the atmosphere for which these simplifications are valid will be discussed later.

The equation of state for a partially dissociated diatomic gas is:

$$p = \frac{R}{M_2}(1+c_1)\rho T \tag{1}$$

where the term $(1+c_1)$ is known as the compressibility factor. For two-dimensional and axisymmetric bodies the boundary-layer conservation equations are:

Mass

$$\frac{\partial(\rho u r^{\epsilon})}{\partial x} + \frac{\partial(\rho v r^{\epsilon})}{\partial y} = 0 \tag{2}$$

Momentum

$$\rho u \frac{\partial u}{\partial x} + \rho v \frac{\partial u}{\partial y} = \frac{\partial}{\partial y}\left(\mu \frac{\partial u}{\partial y}\right) - \frac{dp}{dx} \tag{3}$$

Frozen total energy

$$\rho u \frac{\partial h}{\partial x} + \rho v \frac{\partial h}{\partial y} = \frac{\partial}{\partial y}\left(\frac{\mu}{Pr}\frac{\partial h}{\partial y}\right) + \frac{\partial}{\partial y}\left[\mu\left(1 - \frac{1}{Pr}\right)\frac{\partial}{\partial y}\left(\frac{u^2}{2}\right)\right] \tag{4}$$

Species

$$\rho u \frac{\partial c_i}{\partial x} + \rho v \frac{\partial c_i}{\partial y} = \frac{\partial}{\partial y}\left(\frac{\mu}{Sc}\frac{\partial c_i}{\partial y}\right) \tag{5}$$

where

$$h = \sum_i \left(c_i \int_o^T c_{p,i} dT\right) + \frac{u_e^2}{2} \tag{6}$$

Considerable simplification of the conservation equations results when a new set of independent variables is defined as

$$s = \int_o^x \bar{C} u_e r^{2\epsilon} dx \tag{7}$$

$$t = u_e r^{\epsilon} \int_o^y \frac{\rho}{\rho_{o,e}}\, dy \tag{8}$$

where

$$\bar{C} = \frac{\rho\mu}{\rho_{e,o}\mu_{e,o}} = \left(\frac{\rho\mu}{\rho_e\mu_e}\right)\left(\frac{\rho_e\mu_e}{\rho_{e,o}\mu_{e,o}}\right) = C\left(\frac{\rho_e\mu_e}{\rho_{e,o}\mu_{e,o}}\right) \tag{9}$$

Following references 9 and 10 we assume

$$C = \left(\frac{\rho_{w,o}\mu_{w,o}}{\rho_{e,o}\mu_{e,o}}\right)^{0.2} \tag{10}$$

and

$$\frac{\rho_e\mu_e}{\rho_{e,o}\mu_{e,o}} = \frac{p_e}{p_o} \tag{11}$$

Now $\bar{C}$ is a function of x alone. It was shown in references 9 and 10 that these assumptions (eqs. (10) and (11)) affect the solution for heat transfer to an infinitely catalytic wall or a totally noncatalytic wall by less than 10 percent. It might be expected that discrepancies for intermediate values of catalytic activity will be as small.

Transformation of the conservation equations to the set of independent variables s and t is accomplished by means of the following relations:

$$\frac{\partial(\ )}{\partial x} = \bar{C} u_e r^{2\epsilon} \frac{\partial(\ )}{\partial s} + \frac{\partial t}{\partial x} \frac{\partial(\ )}{\partial t} \tag{12}$$

$$\frac{\partial(\ )}{\partial y} = u_e r^{\epsilon} \frac{\rho}{\rho_{e,o}} \frac{\partial(\ )}{\partial t} \tag{13}$$

A stream function is defined to satisfy the mass conservation equation (2) as

$$\rho u r^{\epsilon} = \rho_{o,e} \frac{\partial \Psi}{\partial y} \tag{14}$$

$$\rho v r^{\epsilon} = -\rho_{o,e} \frac{\partial \Psi}{\partial x} \tag{15}$$

Transformed to the s-t plane, equations (14) and (15) become

$$\frac{u}{u_e} = \frac{\partial \Psi}{\partial t} \tag{16}$$

$$\rho v = -\frac{\rho_{o,e}}{r^{\epsilon}} \left(\bar{C} u_e r^{2\epsilon} \frac{\partial \Psi}{\partial s} + \frac{\partial t}{\partial x} \frac{\partial \Psi}{\partial t} \right) \tag{17}$$

New dependent variables are defined as

$$U = \frac{\partial \Psi}{\partial t} \tag{18}$$

$$V = -\frac{\partial \Psi}{\partial s} \tag{19}$$

Now with the use of equations (7) through (19), the conservation equations (2) through (5) can be transformed to somewhat resemble the familiar incompressible boundary-layer equations as follows:

Mass

$$\frac{\partial U}{\partial s} + \frac{\partial V}{\partial t} = 0 \tag{20}$$

Momentum

$$U \frac{\partial U}{\partial s} + V \frac{\partial U}{\partial t} = \nu_{o,e} \frac{\partial^2 U}{\partial t^2} + \frac{1}{u_e} \frac{du_e}{ds} \left(\frac{\rho_e}{\rho} - U^2 \right) \tag{21}$$

Frozen total energy

$$U \frac{\partial h}{\partial s} + V \frac{\partial h}{\partial t} = \frac{\nu_{o,e}}{Pr} \frac{\partial^2 h}{\partial t^2} + \nu_{o,e} u_e^2 \left(1 - \frac{1}{Pr} \right) \frac{\partial^2}{\partial t^2} \left(\frac{U^2}{2} \right) \tag{22}$$

Species

$$U \frac{\partial c_i}{\partial s} + V \frac{\partial c_i}{\partial t} = \frac{\nu_{o,e}}{Sc} \frac{\partial^2 c_i}{\partial t^2} \tag{23}$$

The last term in equation (21) is zero for a flat plate without pressure gradient. Also, according to reference 9, it may be neglected in a highly cooled hypersonic boundary layer over a blunt body. Equation (21) therefore becomes for a flat plate or a highly cooled hypersonic blunt body

$$U \frac{\partial U}{\partial s} + V \frac{\partial U}{\partial t} = \nu_{o,e} \frac{\partial^2 U}{\partial t^2} \tag{24}$$

Equation (23) may be written, for the diatomic gas under consideration

$$U \frac{\partial c_1}{\partial s} + V \frac{\partial c_1}{\partial t} = \frac{\nu_{o,e}}{Sc} \frac{\partial^2 c_1}{\partial t^2} \tag{25}$$

$$C_2 = 1 - c_1 \tag{26}$$

Note that as a consequence of the assumption of equation (10) the momentum and species conservation equations are no longer coupled to the energy equation; therefore, equation (22) need not be treated here since its solution may be found elsewhere. Equations (20), (24), and (25) are in the form of the familiar incompressible flat plate boundary-layer equations and are now amenable to solutions. Now it is seen that the pertinent original boundary-layer equations (2), (3), and (5) are simplified to equations (20), (24), and (25). The boundary conditions on these equations are as follows:

at $t = 0$:

$$U = 0 , \qquad V = \frac{\rho_w}{\rho_{o,e}\bar{C}u_e r^{\epsilon}} v_w ,$$

$$\frac{\partial c_1}{\partial t} = \frac{\rho_{o,e}\, Sc\, V_w c_{1,w}}{\mu_{o,e}} + \frac{Sc}{\mu_{o,e}\bar{C}u_e r^{\epsilon}} J_{1,w} \qquad (27)$$

at $t = \infty$:

$$U = 1 , \qquad c_1 = c_{1,e}$$

at $s = 0$:

$$\sqrt{s}\left(\frac{\partial U}{\partial t}\right) \rightarrow \text{Bounded} , \qquad \sqrt{s}\left(\frac{\partial m}{\partial t}\right) \rightarrow \text{Bounded} \qquad (28)$$

A425

The boundary conditions are not yet complete since $J_{1,w}$ is not known. The term $J_{1,w}$ is the mass flux of atoms to the wall and is obtained from a consideration of the chemical kinetics of the surface reaction. Therefore, we shall include in the subsequent section a brief discussion of the surface chemical reaction kinetics before going into the actual solution of the equations.

CHEMICAL KINETICS OF THE CATALYTIC SURFACE REACTION

More comprehensive treatments of the subject about to be discussed may be found in references 11 and 12.

It is generally accepted that the catalytic recombination of dissociated air on surfaces at temperatures lower than 2000° K and at pressures above 10^{-4} atm is a first-order process proceeding only toward the negligibly small equilibrium atom concentration. This discussion is limited to such a reaction.

The microscopic reaction rate, which is a function of the rate of collision with the wall, may be obtained as follows for a dissociated diatomic gas: Let $\gamma\chi_2$ be the probability of an atom recombining upon striking the wall. The equilibrium mole fraction of the molecules, χ_2, is unity at the surface temperatures and pressures of interest here. The factor γ is commonly referred to as the "catalytic efficiency." The mass rate of recombination may then be written

$$J_{1,w} = \gamma Z \qquad (29)$$

where Z is the mass rate of collision of atoms with the wall and is, for a Maxwellian distribution,

$$Z = \rho_w c_{1,w} \sqrt{\frac{RT_w}{2\pi M_1}} = p \sqrt{\frac{2M_1}{\pi RT_w}} \left(\frac{c_{1,w}}{1+c_{1,w}} \right) \tag{30}$$

then

$$J_{1,w} = \gamma p \sqrt{\frac{2M_1}{\pi RT_w}} \left(\frac{c_{1,w}}{1+c_{1,w}} \right) \tag{31}$$

In engineering work, including the present analysis, the reaction rate is often written

$$J_{1,w} = k_w \rho_w c_{1,w} = 2k_w \frac{pM_1}{RT_w} \left(\frac{c_{1,w}}{1+c_{1,w}} \right) \tag{32}$$

The specific catalytic rate constant, k_w, is related to the catalytic efficiency by the expression

$$\gamma = \sqrt{\frac{2\pi M_1}{RT_w}} k_w \tag{33}$$

The magnitude and temperature dependency of k_w are not well known for most surfaces; however, metallic and metallic oxide surfaces have much higher efficiencies than nonmetallic surfaces. For instance, at room temperature, k_w for a metallic oxide is about 10 ft/sec, whereas k_w for pyrex is about 0.1 ft/sec (see ref. 6). There are also possibilities of "poisoning" surfaces to reduce their catalytic efficiency. Reference 13 reported a substantial reduction of the catalytic efficiency of metallic surfaces upon application of iodine coatings.

REDUCTION OF GENERAL EQUATIONS TO AN ORDINARY DIFFERENTIAL EQUATION

In this section, the partial differential equations (20), (24), and (25) with the boundary conditions of (27) will be reduced to an ordinary differential equation by the use of an integral method described in reference 14.

The diffusion boundary layer is assumed to have the thickness of the momentum boundary layer, an assumption which is believed to be valid for Sc in the order of 1 according to reference 14. Equations (24) and (25) are integrated across the boundary layer with the aid of equation (20). The resulting integro-differential equations are

$$\lambda F_1' + \frac{F_1}{2}\lambda' = \left(\frac{\partial U}{\partial \eta}\right)_w + \Gamma \tag{34}$$

$$\lambda F_2' + \frac{F_2}{2}\lambda' = \frac{1}{Sc}\left(\frac{\partial m}{\partial \eta}\right)_w + \Gamma\left(1-m_w\right) \tag{35}$$

where

$$\eta = \frac{t}{\delta_t} = \frac{\int_o^y (\rho/\rho_{e,o}dy)}{\int_o^\delta (\rho/\rho_{e,o}dy)} \tag{36}$$

$$\lambda = \frac{\delta_t^2}{\nu_{e,o}} \tag{37}$$

$$\Gamma = \frac{V_w \delta_t}{\nu_{e,o}} \tag{38}$$

$$F_1 = \int_o^1 U(1-U)d\eta \tag{39}$$

$$m = \frac{c_1}{c_{1,e}} \tag{40}$$

$$F_2 = \int_o^1 U(1-m)d\eta \tag{41}$$

and the prime denotes differentiation with respect to s. The boundary conditions become, with the aid of equation (32),

at $\eta = 0$:

$$\left.\begin{aligned} U &= 0 \\ V &= V_w \\ \frac{\partial m}{\partial \eta} &= \Gamma\, Sc\, m + \frac{\rho k_w\, Sc\, \delta_t}{\mu_{e,o}\bar{C}u_e r^\epsilon}\, m \end{aligned}\right\} \tag{42}$$

at $\eta = 1$

$$\left.\begin{aligned} U &= m = 1 \\ \frac{\partial U}{\partial \eta} &= \frac{\partial m}{\partial \eta} = 0 \end{aligned}\right\} \qquad (43)$$

In order to solve equations (34) and (35), the form of U and m profiles must first be assumed. Fourth and fifth degree polynomials in η are chosen to represent the profiles for U and m, respectively.

Thus:

$$U = \sum_{n=0}^{4} a_n \eta^n \qquad (44)$$

$$m = \sum_{n=0}^{5} b_n \eta^n \qquad (45)$$

The coefficients a_n and b_n are obtained by satisfying a sufficient number of boundary conditions at $\eta = 0$ and $\eta = 1$. Equation (44) must satisfy five boundary conditions. One coefficient in equation (45) is left to be determined as the solution of equation (35); therefore, only five boundary conditions are needed. These boundary conditions are those from equations (42) and (43), and those obtained by satisfying equations (24) and (25) at $\eta = 0$ and 1.0. The particular choice of profiles, equations (44) and (45), is justified a posteriori by the close agreement of the present solutions with available exact solutions as will be shown later.

Consider the momentum equation (34). It is well known that an affine solution of the momentum equation exists which satisfies the present boundary conditions when Γ is constant (similarity transpiration). This fact enables us to set $F_1' = 0$, and to rewrite equation (34) as

$$\lambda' = \frac{(\partial U/\partial \eta)_w + \Gamma}{F_1/2} = \text{constant} \qquad (46)$$

Therefore:

$$\lambda = \lambda' s \qquad (47)$$

The catalytic boundary condition described in (42) may be written, with the aid of equations (1), (7), (9), and (47), as

$$\left(\frac{\partial m}{\partial \eta}\right)_w = \Gamma \, Sc \, m_w + G \, Sc \, \Phi \, \frac{m_w}{1+m_w c_{1,e}} \tag{48}$$

where the reaction parameter, G, is

$$G = \frac{(1+c_{1,e})T_{e,o}}{T_w} \left(\frac{k_w}{u_\infty}\right) \sqrt{\frac{\lambda'}{C}} \sqrt{Re_{o,e}} \tag{49}$$

and the shape factor, Φ, is

$$\Phi = \sqrt{\frac{u_\infty s}{CLu_e^2 r^{2\epsilon}}} = \frac{\left[\int_o^x \left(\frac{p_e}{p_o}\right)\left(\frac{u_e}{u_o}\right) r^{2\epsilon} dx\right]^{\frac{1}{2}}}{\sqrt{L}\left(\frac{u_e}{u_\infty}\right) r^{\epsilon}} \tag{50}$$

Upon substitution of the polynomial profiles with appropriate boundary conditions, the concentration integral, (41), becomes

$$F_2 = B_1(1-m_w) - B_2 \left(\frac{\partial m}{\partial \eta}\right)_w \tag{51}$$

where the constants B_1 and B_2 depend on Γ. Equation (35), with the solution of equation (34) incorporated, may now be written as

$$m_w' = \frac{K_3 - K_2 m_w - K_1\left[\left(1 + \frac{2}{\lambda' B_2 Sc}\right)\Gamma + 2\Phi' s\right] \frac{m_w}{1+m_w c_{1,e}}}{2\left[K_2 + K_1 \Phi \frac{1}{(1+m_w c_{1,e})^2}\right] s} \tag{52}$$

where

$$K_1 = \frac{B_2}{B_1} G \, Sc \tag{53}$$

$$K_2 = 1 + \frac{B_2}{B_1} \Gamma \, Sc \tag{54}$$

$$K_3 = 1 - \frac{2}{\lambda' B_1} \Gamma \tag{55}$$

It is now seen that the pertinent conservation equations are reduced to the single equation (52).

SOLUTION FOR THE SURFACE DISTRIBUTION OF ATOM CONCENTRATION

Condition for Application of the Local Similarity Concept

Before actually solving the equation (52), let us examine the possibility of obtaining the surface distribution of atom concentrations by use of the local similarity concept.

In flow past a wall with a finite catalytic activity, a concentration boundary layer develops through which atoms diffuse to recombine on the surface. The resulting steady state atom concentration along the wall is determined by the relative local rates of atom diffusion to the surface and catalytic recombination at the surface. The diffusion rate of the atoms, for a given concentration potential, is determined by the aerodynamics of the flow, characterized here by the momentum and diffusion boundary-layer equations (24) and (25). The consumption rate of atoms at the wall, on the other hand, is controlled by the heterogeneous chemical reaction kinetics discussed earlier. In general, affine solutions of equation (25) can not be obtained to satisfy the catalytic boundary condition of equation (27). This can be seen, for instance, from the fact that the catalytic boundary condition (48) for the integrated form of the diffusion equation, (35), depends upon the variable X explicitly through Φ. According to the present method of solution characterized by the equation (35) and its boundary conditions, one would have a similarity solution which would specify that m_w be independent of X for any body whose geometry and flow characteristics are such that Φ is independent of X. On the other hand, when Φ varies slowly with X, one expects a local similarity solution, explained below, to be valid.

Here, a local similarity solution means that equation (35) is solved locally with the boundary condition (48) applied as though it were not a function of X, however, with Φ being calculated at the point in question. An affine solution can in this way be obtained locally for each position along the body.

In practice, one could make use of already existing affine solutions for a thermal boundary layer over an isothermal flat plate (ref. 15 for instance). This problem is analogous to the present one when the atom concentration at the wall is independent of X. The affine solution yields a relationship between $(\partial m/\partial \eta)_w$ and m_w for a locality which is then solved simultaneously with equation (48) for $m_w(X)$.

The hypersonic pressure distribution and equilibrium heat-transfer distribution are already known for many interesting body shapes. With this information, the validity of the local similarity solution can be qualitatively checked without performing any calculations. The simple relationship given in reference 15, for instance, describes quite accurately the equilibrium heat transfer to two-dimensional and axisymmetric bodies. The function Φ appears, essentially, in the equilibrium heat-transfer equation of reference 15 from which we obtain

$$\frac{q_{w,E}}{q_{w,o,E}} \sim \frac{p_e}{p_o} \frac{1}{\Phi} \tag{56}$$

Equation (56) shows that if the available pressure and equilibrium heat-transfer curves for a particular two-dimensional or axisymmetric body are found to be similar, then the function Φ for the body is a weak function of X. For such a body the distribution of atom concentration along the wall, therefore the catalytic heat transfer, may be obtained simply by using the local similarity concept.

The differential equation (52) will be solved in the following sections for two typical body geometries; flat plate and axisymmetric cone with spherical nose. A solution will be obtained in closed form for the flat plate. The solution for the axisymmetric body will show that the local similarity concept provides a useful approximation.

The universal constants involved in equation (52) are calculated for the three transpiration rates, $\Gamma = 0$, 1.0, and 2.0, and are given below.

Γ	λ'	B_1	B_2(for Sc = 0.72)
0	34.05	0.2429	0.06270
1.0	45.64	.2323	.06457
2.0	58.51	.2244	.06679

Flat Plate With Similarity Transpiration

The body studied in this section is shown in figure 1(a). For two-dimensional flow without pressure gradient, the streamwise variable becomes

$$s = CL_{ue}X \tag{57}$$

also

$$\Phi = \sqrt{X} \tag{58}$$

Equation (52) becomes

$$\frac{dm_w}{dX} = \frac{K_3 - K_2 m_w - \left(2 + \frac{2}{\lambda' B_2\ Sc}\right) K_1 X^{\frac{1}{2}} \frac{m_w}{1+m_w c_{1,e}}}{2\left[K_2 + \frac{K_1 X^{\frac{1}{2}}}{(1+m_w c_{1,e})^2}\right] X} \tag{59}$$

Equation (59) is nonlinear and the general solution cannot be obtained analytically. There are, however, a few limiting cases for which the equation can be integrated readily, and these cases will be investigated first. They are:

1. When the surface is infinitely catalytic.
2. When the surface is totally noncatalytic.
3. When the compressibility factor at the wall, $(1+m_w c_{1,e})$, is sufficiently near 1.

For the first case it is obvious that $m_w = 0$ for all X. When the wall is noncatalytic, the similarity solution of equation (59) is

$$m_w = \frac{K_3}{K_2} \tag{60}$$

When the compressibility factor at the wall, $(1+m_w c_{1,e})$, is sufficiently near 1, equation (59) simplifies to a first-order linear equation

$$\frac{dm_w}{dX} + \left[\frac{K_2 + \left(2 + \frac{2}{\lambda' B_2\ Sc}\right) K_1 X^{\frac{1}{2}}}{2(K_2+K_1 X^{\frac{1}{2}})\, X}\right] m_w = \frac{K_3}{2(K_2+K_1 X^{\frac{1}{2}})\, X} \tag{61}$$

The closed solution to this equation which satisfies the boundary conditions that m_w is finite at $X = 0$ is

$$m_w = \frac{K_3}{K_2} \frac{1 - \left(1 + \frac{K_1}{K_2} X^{\frac{1}{2}}\right)^{-\left(1 + \frac{2}{\lambda' B_2\ Sc}\right)}}{\left(1 + \frac{2}{\lambda' B_2\ Sc}\right) \frac{K_1}{K_2} X^{\frac{1}{2}}} \tag{62}$$

A limiting process, letting $X \to 0$, shows that $m_{w,o} = K_3/K_2$, an expected result since at $X = 0$ there is no time for reaction. Therefore the inert wall solution, equation (60), must be valid.

More exact solutions of the limiting cases corresponding to solutions (60) and (62) are found elsewhere and we shall compare these solutions here. The exact solution for noncatalytic wall with similarity transpiration can be derived from equation (19) of reference 7 as

$$m_w = \frac{1}{1 - F_w Sc \int_0^\infty \left[\frac{F''(\xi)}{F''(0)}\right]^{Sc} d\xi} \tag{63}$$

A 4 2 5

The transpiration rates are related by:

$$F_w = -2 \frac{v_w}{u_e} \sqrt{\frac{\rho_w u_e x}{\mu_w}} = -\frac{2\Gamma}{\sqrt{\lambda'}} \tag{64}$$

For $F_w = -0.5$ (separation occurs at $F_w = -1.2385$) and $Sc = 0.72$, the approximate result according to equation (60) is within 5 percent of the exact solution. The value of the integral in equation (63) was obtained from reference 16.

Now for the case where the compressibility factor at the wall is sufficiently near 1, $\Gamma = 0$, and $(1+c_{1,e})T_e/\sqrt{C}\,T_w = 1$, equation (62) gives the solution to the problem treated in references 1, 4, and 5, where compressibility and transpiration were not taken into account. In terms of the parameter z used in reference 1,

$$z = \frac{k_w L\, Sc\, \rho_e}{0.339 \mu_e} Re^{-\frac{1}{2}} Sc^{-\frac{1}{3}} X^{\frac{1}{2}} \tag{65}$$

the present solution for $Sc = 0.72$ is

$$m_w = \frac{1 - (1+0.458z)^{-2.30}}{1.053z} \tag{66}$$

This solution, equation (66), is compared with other known solutions in figure 2. For $Sc = 0.72$, a good agreement is shown between the present solution and those of references 1 and 5. Equation (66) was presented in reference 8 by the present authors. Slight differences in the constants are due to the use of a different order polynomial approximation in the velocity profile.

The complete solution of equation (59) is obtained numerically by the use of an IBM 704 digital computer. The numerical solutions were obtained for $Sc = 0.72$ and several combinations of K_1 and $c_{1,e}$ at transpiration rates of $\Gamma = 0$, 1.0, and 2.0. A study of these numerical results revealed that for each value of Γ, the solutions were congruent with equation (62) when $\sigma = m_w/m_{w,o}$ was plotted versus $K_1X^{1/2}/K_2(1+c_{1,e})^{\sigma}$. Therefore, the function $K_1X^{1/2}/K_2$ in equation (62) was replaced by $K_1X^{1/2}/K_2(1+c_{1,e})^{\sigma}$ and the following semiempirical closed form solution was obtained for all compressibility factors.

$$\sigma = \frac{m_w}{m_{w,o}} = \frac{1 - \left[1 + \dfrac{K_1X^{\frac{1}{2}}}{K_2(1+c_{1,e})^{\sigma}}\right]^{-\left(1 + \frac{2}{\lambda' B_2\ Sc}\right)}}{\left(1 + \dfrac{2}{\lambda' B_2\ Sc}\right)\dfrac{K_1X^{\frac{1}{2}}}{K_2(1+c_{1,e})^{\sigma}}} \tag{67}$$

Figure 3 shows the close correlation between equation (67) and the results of the numerical solutions of equation (59) for the three transpiration rates.

It is seen in equation (67) that the general solution depends on the two parameters, $K_1X^{1/2}/K_2(1+c_{1,e})^{\sigma}$ and $2/\lambda' B_2\ Sc$ only.

Once the atom wall concentration is known, the catalytic heat transfer, that is, the heat transfer due to diffusion, $q_{d,w}$, is obtained as follows:

$$q_{d,w} = \rho_w k_w c_{1,w} \Delta h^{\circ} = \left(\frac{k_w p M_2}{RT_w}\right) \Delta h^{\circ} \left(\frac{m_w c_{1,e}}{1+m_w c_{1,e}}\right) \tag{68}$$

the total heat transfer is given by

$$q_w = q_{d,w} + q_{c,w} \tag{69}$$

where $q_{c,w}$ is the heat transfer due to ordinary convection, values of which can be obtained elsewhere, such as in references 7 and 9.

Axisymmetric Conical Body With Spherical Nose

In this section, equation (52) will be first solved numerically for the axisymmetric conical body with spherical nose shown in figure 1(b). An approximate solution will also be obtained by the use of the local similarity concept and the two solutions will be compared.

For simplicity, the following approximations used in reference 15 are used here for the inviscid flow properties.

$$\frac{p}{p_o} = \cos^2 X \ , \quad u_e = u_\infty \beta_o X \quad \text{for} \quad X \leqq \theta \tag{70}$$

$$\frac{p}{p_o} = \cos^2 \theta \ , \quad u_e = u_\infty \beta_o \theta \quad \text{for} \quad X \geqq \theta \tag{71}$$

The streamwise variable s becomes for the body

$$s = C u_\infty \beta_o L^3 \int_o^X X \sin^2 X \cos^2 X \, dX \quad \text{for} \quad X \leqq \theta \tag{72}$$

A 4 2 5

$$s = C u_\infty \beta_o L^3 \left\{ \int_o^\theta X \sin^2 X \cos^2 X \, dX + \theta \cos^2 \theta \int_\theta^X [\sin \theta + (X-\theta)\cos \theta]^2 dX \right\} \quad \text{for} \quad X \geqq \theta \tag{73}$$

also the function Φ becomes

$$\Phi = \sqrt{\frac{\int_o^X X \sin^2 X \cos^2 X \, dX}{\beta_o X^2 \sin^2 X}} \quad \text{for} \quad X \leqq \theta \tag{74}$$

$$\Phi = \sqrt{\frac{\int_o^\theta X \sin^2 X \cos^2 X \, dX + \theta \cos^2 \theta \int_\theta^X [\sin \theta + (X-\theta)\cos \theta]^2 dX}{\beta_o \theta^2 [\sin \theta + (X-\theta)\cos \theta]^2}} \quad \text{for} \quad X \geqq \theta \tag{75}$$

Now to remove a flight condition from the shape factor let

$$\bar{\Phi} = \sqrt{\beta_o}\, \Phi \tag{76}$$

and also define

$$\bar{K}_1 = \frac{K_1}{\sqrt{\beta_o}} = \frac{B_2}{B_1} \, Sc \, \frac{G}{\sqrt{\beta_o}} = \frac{B_2}{B_1} \, Sc \, \bar{G} \tag{77}$$

Now with the aid of equations (70) through (77), equation (52) becomes

$$\frac{dm_w}{dX} = \frac{1 - m_w - 2\overline{K}_1\bar{\Phi}\left(1 + \frac{1}{\lambda' B_2\, Sc} - \bar{\Phi}^2\frac{\sin X + X\cos X}{\sin X\cos^2 X}\right)\frac{m_w}{1+m_w c_{1,e}}}{2\left[1 + \frac{\overline{K}_1\Phi}{(1+m_w c_{1,e})^2}\right]\frac{\bar{\Phi}^2 X}{\cos^2 X}}$$

for $X \leqq \theta$ (78)

$$\frac{dm_w}{dX} = \frac{1 - m_w - 2\overline{K}_1\bar{\Phi}\left\{1 + \frac{1}{\lambda' B_2\, Sc} - \frac{\bar{\Phi}^2\theta}{\cos\theta[\sin\theta + (X-\theta)\cos\theta]}\right\}\frac{m_w}{1+m_w c_{1,e}}}{2\left[1 + \frac{\overline{K}_1\bar{\Phi}}{(1+m_w c_{1,e})^2}\right]\frac{\bar{\Phi}^2\theta}{\cos^2\theta}}$$

for $X \geqq \theta$ (79)

The solution of equation (78) for $X = 0$ (stagnation point) can be obtained from the general local similarity solution of equation (35). This solution is for $\Gamma = 0$

$$m_w = \frac{-(\Omega + 1 - c_{1,e}) + \sqrt{(\Omega + 1 - c_{1,e})^2 + 4c_{1,e}}}{2c_{1,e}} \tag{80}$$

where

$$\Omega = \overline{K}_1\left(1 + \frac{2.}{\lambda' B_2\, Sc}\right)\bar{\Phi} \tag{81}$$

The value of Ω at the stagnation point is found by noting

$$\lim_{X\to 0}\bar{\Phi} = 1/2$$

Equation (80) was found to yield stagnation point values which check within 5 percent of the exact solution given in reference 6.

For the region downstream of the stagnation point equations (78) and (79) were integrated numerically for $Sc = 0.72$ and several values of $\overline{G}$ and $c_{1,e}$, and with θ equal to 50° and 70°. These results are shown in figure 4. The solutions for $\overline{G} = 0$ and $\overline{G} = \infty$ represent the two extremes of catalytic activity.

Now let us examine the possibility of using the local similarity solution everywhere along the body. In order to estimate the accuracy of the local similarity solution, the hypersonic pressure and equilibrium heat-transfer distributions (obtained from ref. 15) are shown below for the body in question.

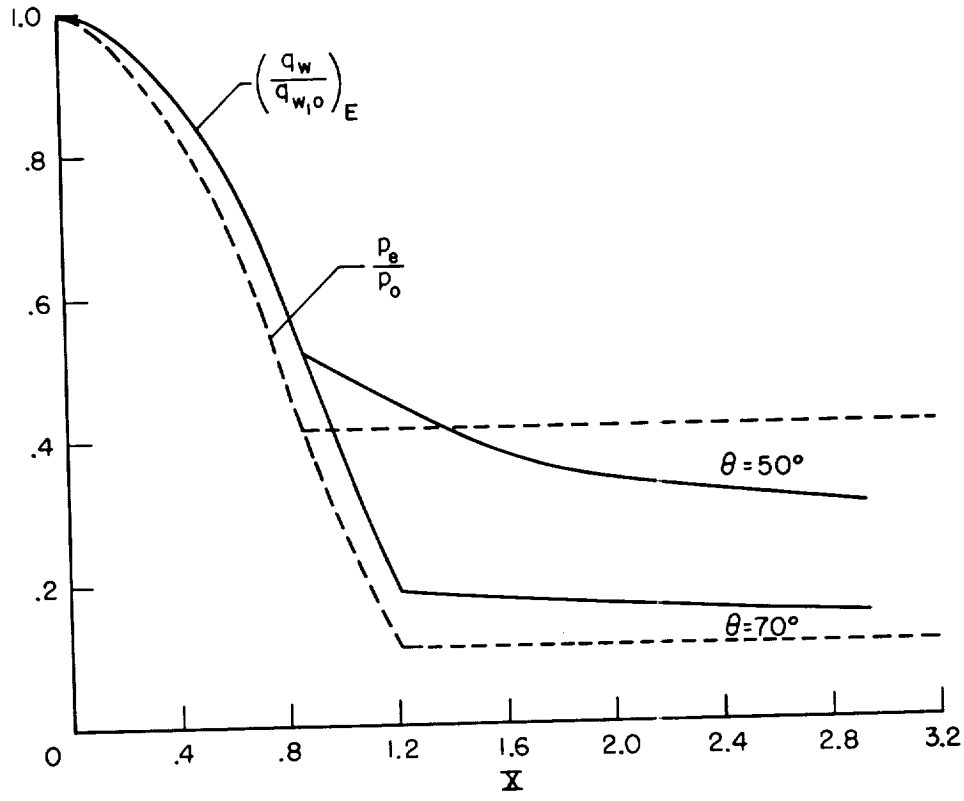

Sketch (a)

Since the curves are quite alike except along the conical afterbody for $\theta = 50^\circ$, equation (80) is expected to be generally quite satisfactory in the determination of the atom wall concentration.

From figure 4 we see that the variation of m_w with X becomes less pronounced as $\bar{G}$ approaches either of the two extremes. The error introduced by a local similarity assumption should therefore be largest at intermediate values of $\bar{G}$, and if its use can be justified there, it should be valid for all values of $\bar{G}$.

Figure 5 shows the catalytic heat transfer based on the numerical solution and the local similarity solution for an intermediate value of the reaction parameter $\bar{G} = 5.0$ and $c_{1,e} = 1.0$. The agreement between the two results is strikingly good, with some deviation along the conical afterbody for $\theta = 50^\circ$ as expected. It seems that the local similarity solution is quite adequate for the calculation of catalytic heat transfer to this body.

APPLICATION TO HYPERSONIC FLIGHT

Altitude Range of Application

As flight altitude is increased, the boundary layer surrounding a hypersonic vehicle passes through a regime in which homogeneous recombination is significant into one where this reaction is frozen and, finally, with very low density, into a regime where the classical boundary-layer theory is no longer valid. The present analysis is applicable in the intermediate regime, that of near frozen boundary-layer flow, where catalytic recombination is probably most significant in the calculation of heat transfer.

Heat transfer to blunt bodies with nonequilibrium boundary layers was considered in reference 17, where it is shown that the boundary layer at the stagnation point becomes practically frozen at about 200,000 feet altitude, depending, of course, on the nose radius and wall temperature. Also, for a particular nose radius and wall temperature, the boundary layer on the conical afterbody will be frozen at considerably lower altitudes.

As the Reynolds number decreases with increasing altitude, the vorticity in the inviscid flow generated by the bow shock becomes comparable to the vorticity in the boundary layer. This is called the vorticity interaction regime, in which it is necessary to modify the classical boundary-layer theory.

Reference 18 indicates that the boundary-layer concept is valid near the stagnation point of a blunt body whenever $M_\infty/Re_\infty \ll \rho_\infty/\rho_{O,e}(\delta/\Delta)$. Consider a hypersonic body of 1 foot radius flying at an altitude of 250,000 feet. The ratio, M_∞/Re_∞, is about one order of magnitude smaller than $\rho_\infty/\rho_{O,e}$, which suggests that boundary-layer theory can still be approximately applied at this altitude. The effect of vorticity interaction on ordinary convective heat transfer to the stagnation point was analyzed in reference 18 for a compressible inert gas. It can be calculated from this analysis that the vorticity interaction effect on heat transfer to the stagnation point of a sphere at the altitude of 250,000 feet is to increase the heat transfer about 10 percent. Since the vorticity in the boundary layer increases rapidly as the gas flows around the body, the altitude at which the vorticity interaction effect becomes important on the conical afterbody should be considerably higher. The present analysis should therefore be applicable between about 200,000 feet and 250,000 feet, a range which may be extended considerably in both directions if one is primarily interested in the conical afterbody.

Discussion of Gas Model

Air, for the present flight range, is more validly described as a mixture of oxygen and nitrogen than as a single diatomic gas. It is felt however, that since the transport properties are quite alike, any important difference, as regards catalytic heat transfer, would be in the reaction rates and heats of reaction.

The conservation of species equation when written independently for oxygen and nitrogen would be identical and when combined, would give equation (35). Now, if k_w were the same for both oxygen and nitrogen, the combined catalytic boundary condition would be the same as that for a single diatomic gas, equation (48). The assumption of equal values of k_w seems reasonable in view of the limited knowledge of heterogeneous reaction rates (ref. 6), and is made here.

With these limitations, equal transport properties and equal values of k_w, the combined atom wall concentration, may be calculated using the present method.

If the solution had been carried out independently for oxygen and nitrogen, with the above assumptions, the reduced concentration profile would be the same for both since the equations are identical with identical boundary conditions. The heat of recombination at the wall Δh^o may therefore, in the present analysis, be obtained as a weighted average based on the atom concentrations at the boundary-layer edge.

The Effect of Catalytic Activity on Hypersonic Heat Transfer

For a given hypersonic blunt body, the catalytic heat transfer is largely controlled by the reaction parameter $\bar{G}$ as can be seen from the general equation (52). Approximate values of $\bar{G}$ for two typical surface materials are shown in figure 6 for the range of flight conditions of interest. The calculations are for the blunt body shown in figure 1 with a nose radius of 1 foot. The values of k_w are taken from reference 6.

The atom diffusion rate into the wall is approximately proportional to the driving potential, $c_{1,e} - c_{1,w}$. Therefore, for $m_w = 0$, $q_{d,w}$ is maximum and the total heat transfer would be about the same as that for an equilibrium boundary layer. The proportion of dissociation energy transferred to the wall will decrease with $(1-m_w)$. Now let us consider a metallic oxide surface, which is quite highly catalytic. It is seen from figures 4 and 6 that at lower altitudes (less than 150,000 ft) the total heat transfer, q_w, will be about as large as equilibrium heat transfer. At the altitude of 250,000 feet, however, the catalytic heat transfer will be reduced by about 50 percent. Since, at high speeds, as much

as 75 percent of the total energy could be associated with dissociation, the total heat transfer would be reduced to about 65 percent of equilibrium heat transfer, even for this highly catalytic surface. Any surface material with a lower catalytic efficiency, such as pyrex, would, of course, reduce the heat transfer to a much lower value.

CONCLUDING REMARKS

The catalytic heat transfer to the surfaces of two-dimensional and axisymmetric bodies with finite catalytic activities was analyzed.

An integral method was used to obtain catalytic heat-transfer predictions to (1) a flat plate in frozen compressible flow with and without transpiration and (2) an axisymmetric conical body with a spherical nose in frozen hypersonic compressible flow without transpiration.

The solution for a flat plate was derived in closed form.

It was shown that for a body whose pressure and equilibrium heat transfer distribution curves are similar, the catalytic heat transfer to the body can be calculated quite accurately by the use of a simple local similarity concept. For the axisymmetric conical body with spherical nose, the pressure and the equilibrium heat-transfer distribution patterns were found to be quite similar. A comparison of the catalytic heat-transfer solution based on the simple local similarity concept with that obtained by the numerical solutions showed that the maximum error was in the order of 5 percent for this body.

It was shown that at high flight altitudes, the dissociation energy would not be recovered completely even with highly catalytic surfaces, such as a metallic oxide. The total heat transfer, therefore, may be considerably less than the equilibrium value for most engineering materials.

Ames Research Center
National Aeronautics and Space Administration
Moffett Field, Calif., Sept. 22, 1960

REFERENCES

1. Chambré, Paul L., and Acrivos, Andreas: On Chemical Surface Reactions in Laminar Boundary Layer Flows. Jour. Appl. Phys., vol. 27, no. 11, Nov. 1956, pp. 1322-1328.

2. Acrivos, Andreas, and Chambré, Paul L.: Laminar Boundary Layer Flows with Surface Reactions. Ind. Eng. Chem., vol. 49, no. 6, June 1957, pp. 1025-1029.

3. Chambré, Paul L.: On Chemical Surface Reactions in Hydrodynamic Flows. Appl. Sci. Res., sec. A, vol. 6, no. 2-3, 1956, pp. 97-113.

4. Rosner, Daniel E.: Chemically Frozen Boundary Layers with Catalytic Surface Reaction. Jour. Aero/Space Sci., vol. 26, no. 5, May 1959, pp. 281-286.

5. Rosner, Daniel E.: Diffusion and Chemical Surface Catalysis in Flow Systems. Tech. Pub. No. 14. AeroChem. Research Labs. Inc., Princeton, N. J., Sept. 1959.

6. Goulard, Robert J.: On Catalytic Recombination Rates in Hypersonic Stagnation Heat Transfer. Jet Propulsion, vol. 28, no. 11, Nov. 1958, pp. 737-745.

7. Chung, Paul M.: Shielding Stagnation Surfaces of Finite Catalytic Activity by Air Injection in Hypersonic Flight. NASA TN D-27, 1959.

8. Chung, Paul M., and Anderson, Aemer D.: Surface Recombination in the Frozen Compressible Flow of a Dissociated Diatomic Gas Past a Catalytic Flat Plate. ARS Jour., vol. 30, no. 3, Mar. 1960, pp. 262-264.

9. Lees, Lester: Convective Heat Transfer With Mass Addition And Chemical Reactions. Third AGARD Combustion and Propulsion Panel Colloquim, Palermo, Sicily, Mar. 17-21, 1958. Pergamon Press, N. Y., pp. 451-498.

10. Kemp, Nelson H., Rose, Peter H., and Detra, Ralph W.: Laminar Heat Transfer Around Blunt Bodies in Dissociated Air. Jour. Aero/Space Sci., vol. 26, no. 7, July 1959, pp. 421-430.

11. Rosner, Daniel E.: Boundary Conditions For the Flow of Multicomponent Gas. Jet Propulsion, vol. 28, no. 8, pt. 1, Aug. 1958, pp. 555-556.

12. Scala, Sinclaire M.: Hypersonic Stagnation Point Heat Transfer to Surfaces Having Finite Catalytic Efficiency. Proc. U.S. Natl. Congress of Appl. Mech. 1958, pp. 799-806.

13. Cutting, John C., Fay, James A., Hogan, William T., and Moffatt, W. Craig: A Non-catalytic Surface for Dissociated Combustion Gases. Preprint, Confer. on Physical Chem. in Aero. and Space Flight, Sept. 1-3, 1959.

14. Morduchow, Morris: Analysis and Calculation by Integral Methods of Laminar Compressible Boundary Layer With Heat Transfer and With and Without Pressure Gradient. NACA Rep. 1245, 1955.

15. Lees, Lester: Laminar Heat Transfer Over Blunt-Nosed Bodies at Hypersonic Flight Speeds. Jet Propulsion, vol. 26, no. 4, Apr. 1956, pp. 259-269.

16. Low, George M: The Compressible Laminar Boundary Layer with Fluid Injection. NACA TN 3404, 1955.

17. Chung, Paul M., and Anderson, Aemer D.: Heat Transfer Around Blunt Bodies with Nonequilibrium Boundary Layers. Proc. 1960 Heat Transfer and Fluid Mechanics Institute.

18. Hayes, Wallace D., and Probstein, Ronald F.: Hypersonic Flow Theory. Academic Press, New York, 1959, pp. 370-386.

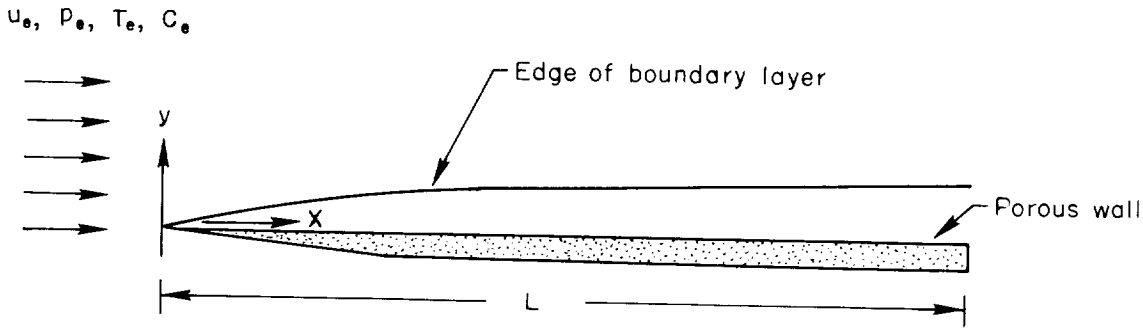

(a) Flat plate

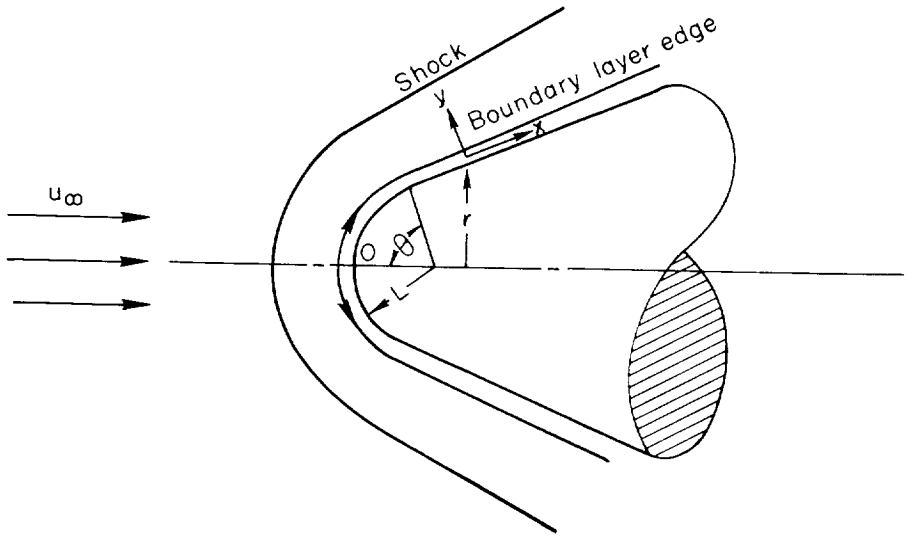

(b) Axisymmetric cone with spherical nose

Figure 1.- Physical models considered.

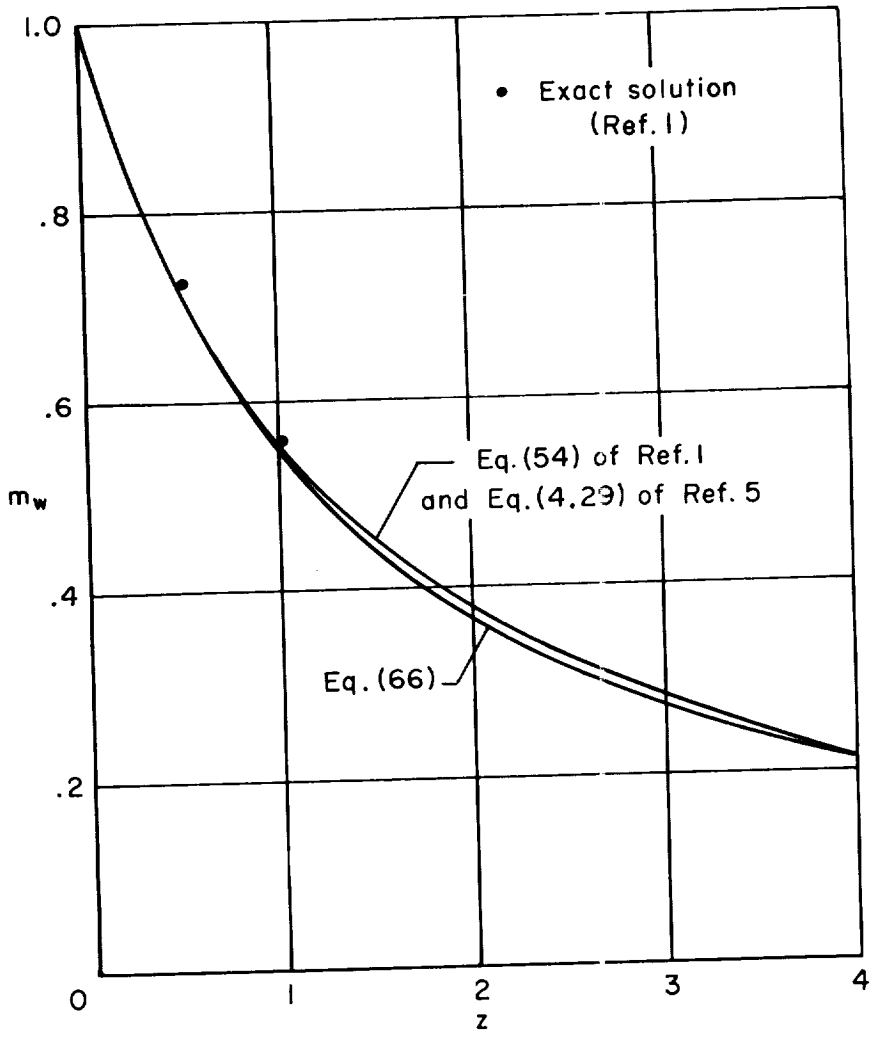

Figure 2.- Incompressible solutions for $\Gamma = 0$.

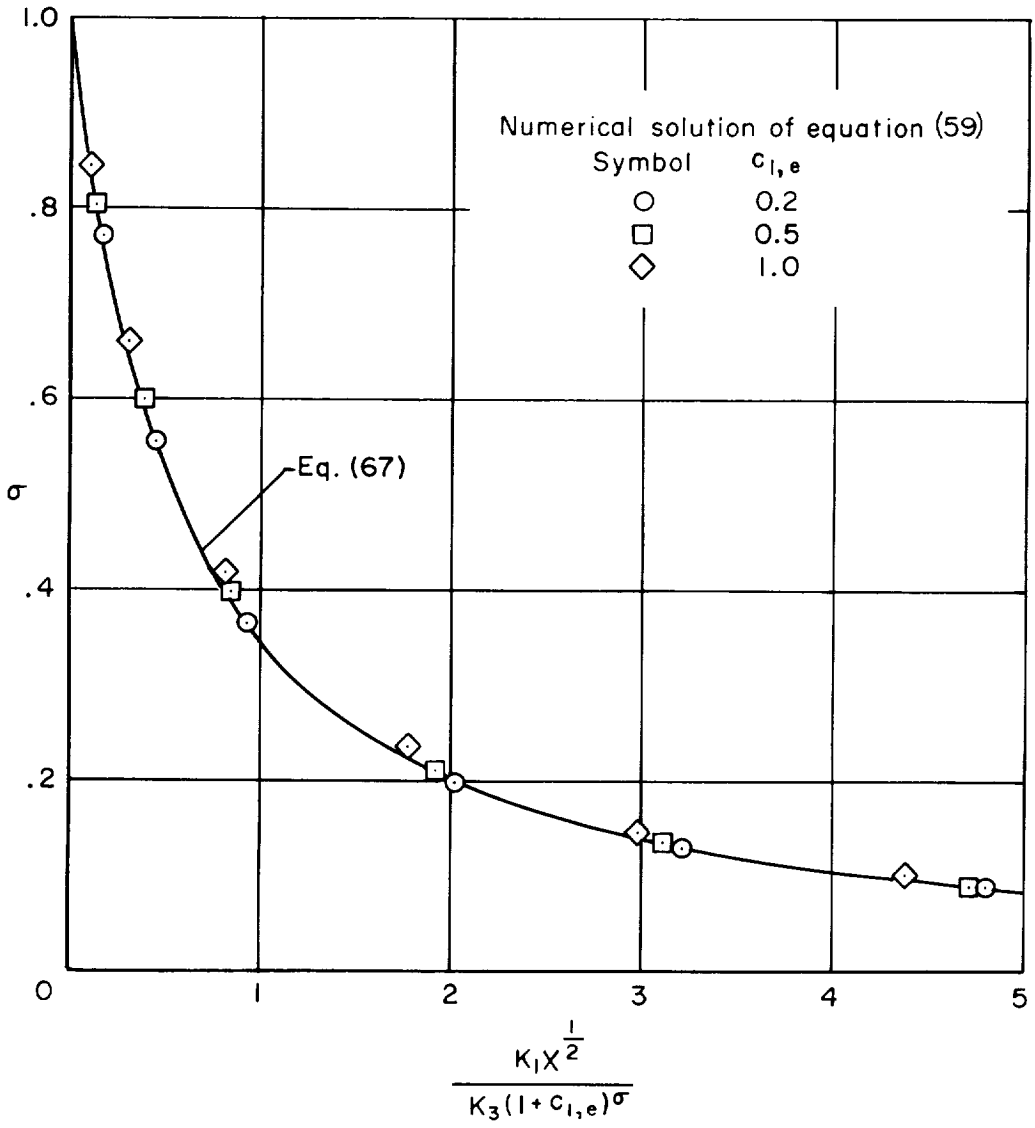

(a) $\Gamma = 0$

Figure 3.- Correlation of equation (67) with numerical solutions.

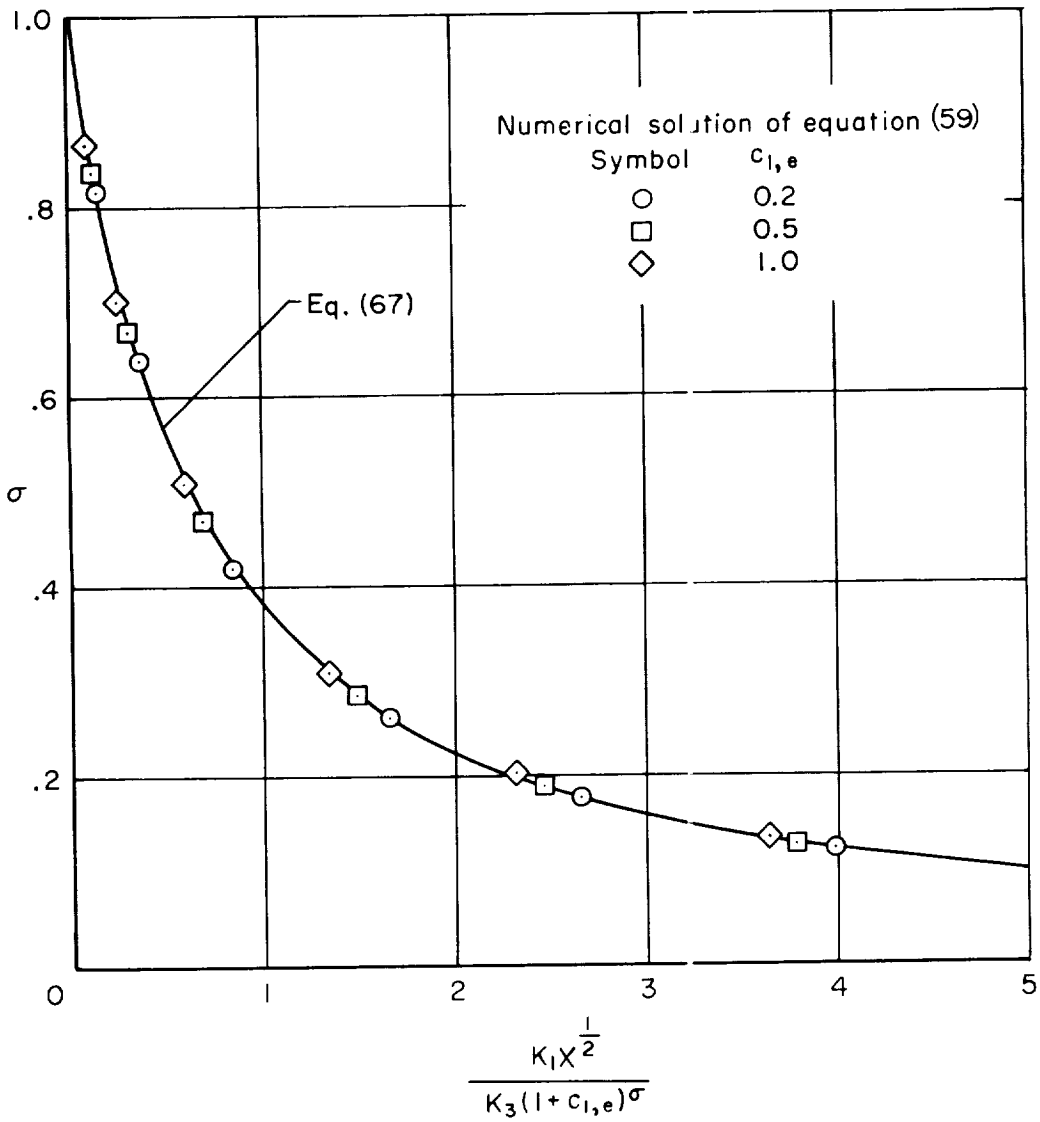

(b) $\Gamma = 1.0$

Figure 3.- Continued.

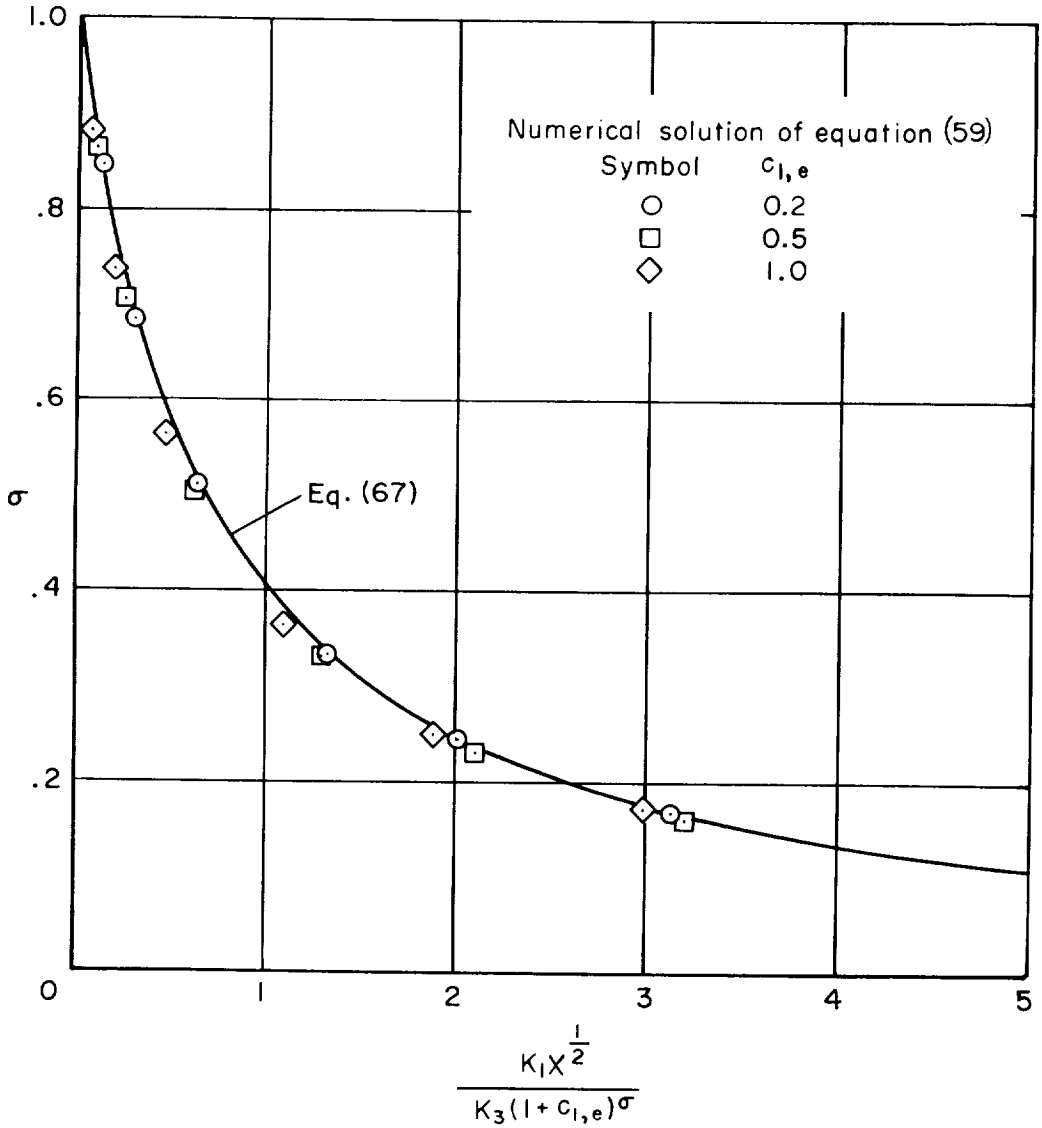

(c) $\Gamma = 2.0$

Figure 3.- Concluded.

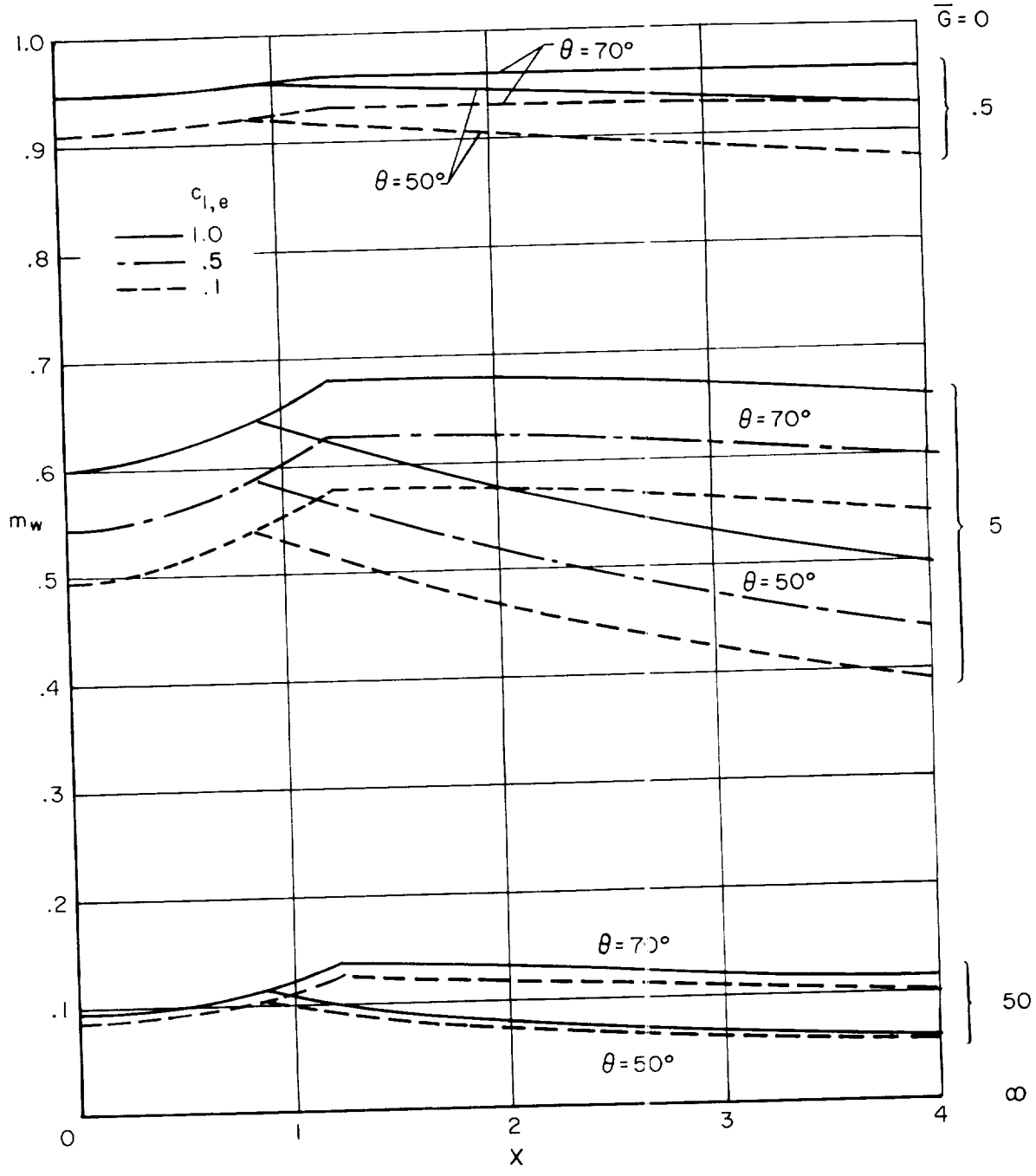

Figure 4.- Atom distribution along axisymmetric cone with spherical nose.

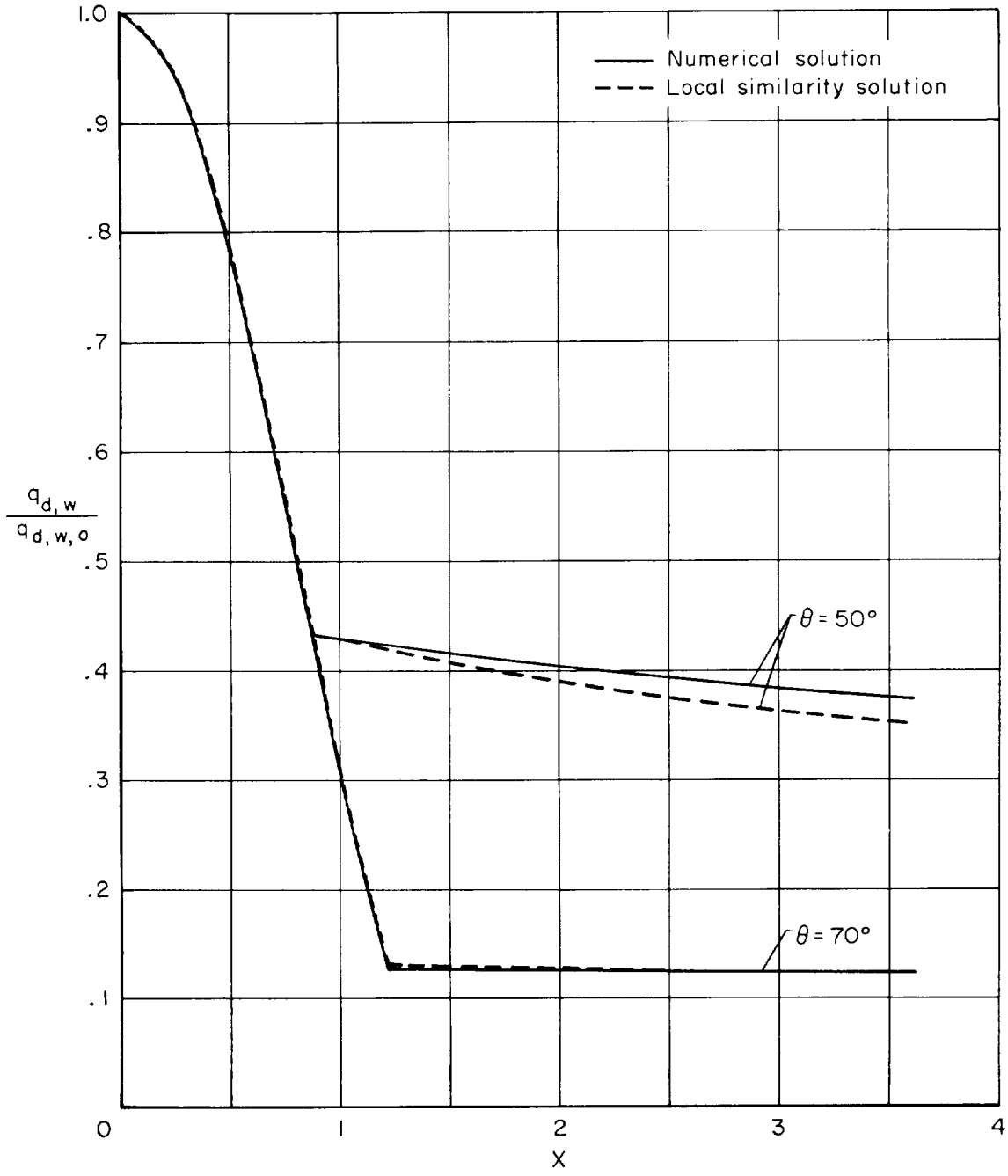

Figure 5.- Catalytic heat transfer around the axisymmetric cone with spherical nose.

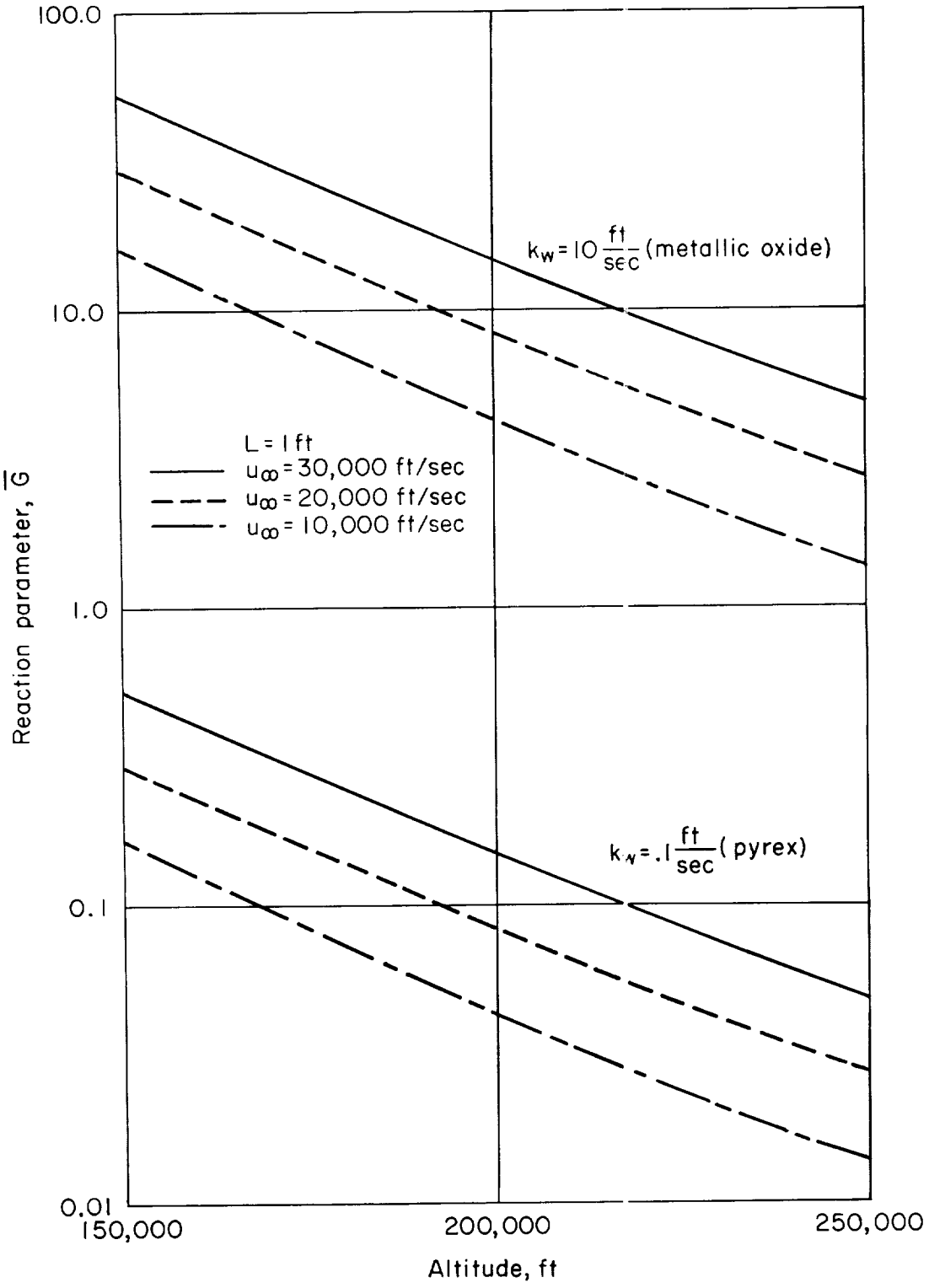

Figure 6.- Variation of reaction parameter with flight condition.